Science of Sintering, **54** (2022)415-424

https://doi.org/10.2298/SOS2204415A

UDK: 692.533.1; 595.43

Fabrication of an Al_2O_3-1% Ti Composite with some Characteristics of a Biomaterial

Ruth P. Alvarez-Carrizal[1], Elizabeth Refugio-García[2], José A. Rodríguez-García[1], José G. Miranda Hernández[3], Enrique Rocha-Rangel[1*)]

[1]Manufacture Department, Universidad Politécnica de Victoria, México
[2]Materials Department, Universidad Autónoma Metropolitana, México
[3]Industrial Materials Research and Development Laboratory, Universidad Autónoma del Estado de México, Centro Universitario UAEM Valle de México, México

Abstract:

An Al_2O_3-1 wt.% Ti composite was prepared by powder techniques with the intention of analyzing its mechanical and chemical properties for its possible application as a biomaterial. Alumina was synthesized using the reaction bonding aluminum oxide (RBAO) process. The powders resulting from the milling stage present sizes minor than 1.5 microns. With the help of X-ray diffraction and differential thermal analysis, it was determined that aluminum oxidizes in both solid and liquid states during the RBAO process. It was also found that the alumina formation reaction in this process is completed at 1,100°C. From the measurements of mechanical properties (HV, KIC, E) in the Al2O3-1 wt.% Ti composite, it was determined that these properties are better than the same properties of compact bone. Electrochemical impedance spectroscopy, indicates that additions of 1 wt.% Ti on Al_2O_3 enhance its corrosion resistance. The bioactivation of a Al_2O_3-1 wt.% Ti composite was successful using a biomimetic method, because after 21 days, hydroxyapatite begins to proliferate on the surface of the substrate. With all these results it can be commented that it is feasible to use Al_2O_3-1 wt.% Ti composite in the elaboration of synthetic bone for its application as a biomaterial.

Keywords*: Alumina; Titanium; Bioactivation; Biomaterial; Compact bone.*

1. Introduction

Among the many applications of composite materials in the aeronautics, automotive, space, sports and medical industries, the latter currently has a wide range of well-defined applications and others that are under development for possible use as structural biomaterials. Biomaterials are useful for many applications like joint replacements, bone plates, bone cement, artificial ligaments as well as tendons and artificial tissue. There are different composite biomaterials currently used, which can be of polymeric, metallic or ceramic matrices, generally reinforced with carbon fibers, metallic particles, ceramic particles and a combination of these. Biomaterials with a ceramic matrix can be reinforced with polymers or metals, since the ceramic matrix provides biocompatibility, hardness and good wear and corrosion resistance. Biocomposites can be prepared with different ceramics, metals and polymer matrices [1-7] which, when reinforced with polymers and metals, reduce their elastic

*) **Corresponding author:** erochar@upv.edu.mx

modulus, making it closer to that of real bone, thus reducing the stresses generated in the joints between the implant and the bone. However, the processes by which these composites are manufactured are by extrusion, generating that these composites present low values of fracture toughness, reliability and mechanical resistance, causing tribological anomalies, that is to say, superficial wear of these biocomposites and in some occasions the definitive rupture of the material, so that, the fracture toughness, mechanical resistance and wear are important factors that define the durability of a biomaterial to be used as a prosthesis, so we have to look at new composite materials whose processing routes allow to improve these properties.

One of those ceramics considered as suitable candidates to manufacture biocompatible composite materials is Al_2O_3 which is a material that has a high resistance to wear at both low and high temperatures and a good resistance to wear in corrosive environments [8]. However, the mechanical properties of alumina, mainly its fracture toughness, are very low (~3 $MPam^{1/2}$), which has greatly limited its applications, mainly in human body components such as bones, where high fracture toughness values are required. Thus, there has been a series of researches in which the fracture toughness of alumina and some other ceramics has been improved through the addition of metallic particles, thus producing composite materials with possible applications as biomaterials. Such is the case of Yoshida [9] who studied the mechanical properties of a ZrO_2/stainless steel composite with contents of up to 30 % by volume of metal, with this concentration they were able to increase the toughness (K_{IC}) up to 6 $MPam^{1/2}$. Mishina has evaluated the mechanical properties of this same system with gradient function, reaching toughness values up to 14 $MPam^{1/2}$[10]. However, in both cases, biocompatibility problems were encountered due to the toxicity of steel. Yao et al, succeeded in fabricating Al_2O_3-Ni composites using spark plasma sintering, obtaining fracture toughness values of 3.84 $MPam^{1/2}$[11]. Konopka has studied the Al_2O_3-Mo system obtaining fracture toughness values of 4.84 to 6.62 $MPam^{1/2}$[12]. Similarly, Lucchini has reported fracture toughness values of 6, 9 and 12 $MPam^{1/2}$ for molybdenum contents of 15, 20 and 25 % by volume [13]. On the other hand, De Portu has fabricated Al_2O_3-Nb composites by hot compaction under vacuum in a graphite die, obtaining values of 5.2 $MPam^{1/2}$ [14]. Pérez de la Fuente, using traditional powder techniques, studied Al_2O_3-Ag composites, achieving fracture toughness values of 8-10 $MPam^{1/2}$[15]. Jia has found that the addition of Fe_3Al in an Al_2O_3 matrix conferred good ductility properties, low density and high oxidation and corrosion resistance, obtaining toughness values of 4.1, 5.7, 8.1 $MPam^{1/2}$, and fracture toughness values of 633, 749 and 860 MPa, respectively, for different intermetallic contents [16]. Picornell has carried out a research where through powder metallurgy they manufactured a hydroxyapatite/Ti composite, where they indicate that it is possible to obtain values of E=22-31 GPa, which are the closest to the values of the elastic modulus of human bone (E=10-30 GPa) [17]. In turn, Maji has conducted a study, where their objective was to improve the mechanical, structural and hydrothermal stability properties of Al_2O_3/ZrO_2 composites for biomedical applications, achieving toughness values of 5.1 $MPam^{1/2}$[18]. Finally, Liu Jian has fabricated Al_2O_3/ZrO_2 composites by hot isostatic compaction, with fracture toughness of 5.2 $MPam^{1/2}$ approximately [19]. Titanium is a metal with biocompatibility characteristics which has been used in the manufacture of different biomaterials to be implanted in the human body [20,21]. Thus, trying to take advantage of the biocompatibility of alumina and titanium, this work seeks to manufacture a biomaterial that combines the mechanical properties of alumina and the toughness of titanium through the powder metallurgy technique, which is a simple and relatively inexpensive method.

2. Materials and Experimental Procedures

An Al_2O_3-1 wt.% Ti composite was prepared using titanium (Aldrich, purity: 99.99 %, 5-10 μm), aluminum (Aldrich, purity: 99.99 %, 5-10 μm) and alumina (Aldrich,

purity: 99.99 %, 1 μm). The 30% of the alumina used for the preparation of composite was synthesized using the RBAO process (reaction 1), method by means of which Al_2O_3 nanometric particles can be obtained from the oxidation of metallic Al [22]. The grinding of the powders was carried out in two stages, in the first (oxidizing stage) only the Al + Al_2O_3 mixture was ground. These powders were subjected to an oxidation heat treatment (RBAO process), heated at 2 ^oC/min to 1.100^oC and left at that temperature for 1 hour and then cooled. The second milling was carried out with the powders resulting from the oxidizing stage plus Ti aggregates. Each milling stage was carried out by a high energy milling process, in a planetary type mill (Retsch, PM100 German), using isopropyl alcohol as a control agent; ZrO_2 spheres of 10 mm in diameter were used as grinding media; the grinding time was 3 h and carried out at 300 rpm. After the grinding of the powders, their size and particle size distribution were determined with a Mastersizer 2000, England equipment. To follow the transformation sequence of the reagents (Al + Al_2O_3) after first grinding, interrupted tests were carried out in an electric furnace (Thermo Scientific Thermolyne FB1315M, USA) at different temperature (450, 600, 750, 900 and 1100^oC), at atmospheric pressure. For this purpose, powders were heated at a speed of 2 ^oC/min to the desired temperature and cooled down inside the furnace. After heating, to determine the crystalline species present in the sample, all powders were analyzed by X-ray diffraction (Panalytical x'pert pro, Japan). To follow the progress of reaction 1, a sample of the first powder mixture was subjected to thermogravimetric analysis in a Shimadzu, DTG-60-H, Japan equipment. The powders resulting from the second grinding were molded by uniaxial compaction at 350 MPa (Montequipo, LAB-30-T, Mexico), into cylindrical pellets of 2 cm in diameter by 0.3 cm thick. Conformed samples were then subjected to a sintering treatment for 2 h at 1500^oC, in an electric furnace (Carbolite, RHF17/3E, England) with a protective atmosphere of argon. Before the characterization of the sintered composite, it was prepared by SiC papers grinding and polishing using 3 μm and 1 μm diamond suspension. Then physical characterization of the composite was carried out to determine the density and interconnected porosity, according to the Archimedes' principle [23]. To determine the crystalline phases of the sintered composite, an X-ray diffraction study was carried out. For the identification of the diffraction peaks, the obtained diffractograms were compared with the charts available in the PCPDFWIN database. Fracture toughness was obtained by the indentation fracture technique using the Miyoshi's equation [24]. The hardness and elastic modulus also were determined according to standards [25,26]. The microstructural characteristics of the composite was observed by SEM (JEOL, JSM 6300, Japan). Corrosion susceptibility studies were carried out on the studied materials by means of electrochemical impedance spectroscopy (EIS) assisted by potentiodynamic polarization techniques carried out in a Potentiostat-Galvanostat, VersaSTAT-4, USA, equipment. Finally, the re-immersion method was used to promote bioactivity on the composite. The solutions were prepared according to what Kokubo mentions in his publication [27], using two simulated biological fluids, one with an ionic concentration similar to that of human blood plasma (SBF) and the other 40 % more concentrated (1.4 SBF).

$$2Al + 3/2O_2 + \underset{\text{(seed-old alumina)}}{Al_2O_3} \rightarrow \underset{\text{(new alumina)}}{Al_2O_3} \qquad (1)$$

3. Results and Discussion

3.1 Particle size distribution

The cumulative distribution for the powders resulting from the second milling stage is reported in Fig. 1. For a better interpretation of this figure, deciles D10, D50 (median), and D90 were taken, from this figure we have that the accumulated size of particle in the first

decile (D10) is approximately 1.4 microns; for the median (D50), we have an accumulated distribution of approximately 1.7 microns in the particle size and for the decile D90 the accumulated distribution of particle size is 2.4 microns. Of these results, in the 50 % of the accumulated volume of particles' size distribution, the particle size is 1.5 microns, which should be suitable for the sintering stage because there is a smaller separation distance between particles, which favors the atomic diffusion process during sintering. Consequently, well-densified bodies with homogeneous microstructure can be obtained, which should be favorable for mechanical properties.

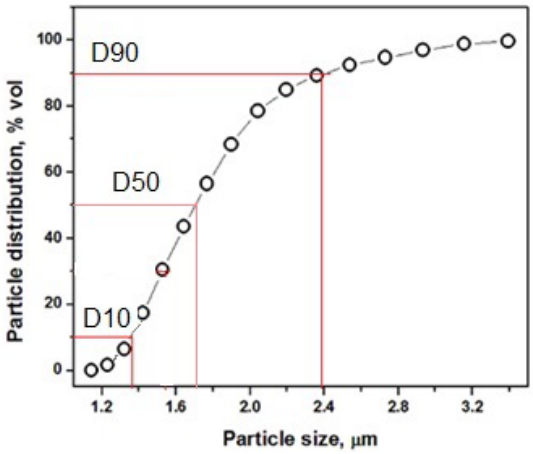

Fig. 1. Particle size distributions after 2 do milling stage.

3.2 Thermogravimetric analysis

A thermogravimetric analysis was performed on powders resulting from the first milling stage in order to follow the sequence of aluminum oxidation in agreement with reaction (1) see Fig. 2. This figure shows that from the beginning of the process and up to 500°C there was no change in the weight of the sample. However, from this point on, a slight gain in weight begins due to the start of the aluminum oxidation reaction, which at this temperature is still in the solid state, when reaching the temperature of 660°C, aluminum reaches its melting temperature and it is here where there begins to be a considerable gain in weight. Complete oxidation reaction ends approximately at 900°C. Thus, from the beginning of the reaction until its completion, there was a weight gain of 9.8 %, which corresponds to the introduction of oxygen to the sample by the oxidation of aluminum to form new alumina (RBAO process).

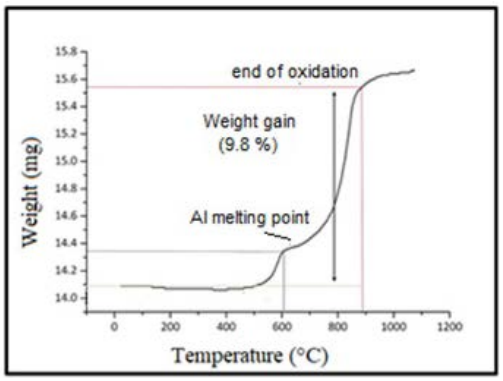

Fig. 2. Thermogravimetric analysis on powders from the first milling stage.

3.3 X-ray diffraction (Interrupted tests and sintered sample)

The progress of the aluminum oxidation reaction (RBAO process) was also monitored by X-ray diffraction. Fig. 3 shows the diffraction patterns of samples subjected to interrupted heating tests at different temperatures. In pattern (a-450^{o}C), there are particles of both alumina and aluminum distributed throughout the sample. As it can be observed in pattern (b-600^{o}C), the intensity of the aluminum peaks is decreasing, this is because it begins to transform into alumina. As shown in pattern (c-750^{o}C), this transformation continues to be observed, until reaching almost the culmination of the reaction in the pattern (d-900^{o}C), where only a small aluminum peak can be seen. In pattern (e-1100^{o}C), it can be seen how the aluminum oxidation reaction was successfully carried out, since there was only alumina in the sample. Finally, pattern (f-1500^{o}C) associated with the sintered sample, in this pattern principally it can be see the crystalline structures corresponding to Al_2O_3 and Ti, however, also there is the presence of a small peak that corresponds to Al_2TiO_5, this means that some small of Ti has oxidized during the sintering of the composite.

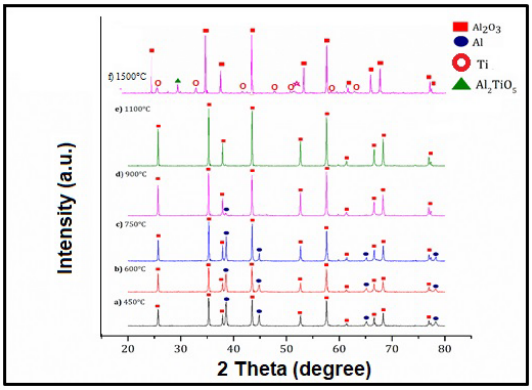

Fig. 3. X-ray diffraction patterns of interrupted heating test.

3.4 Microstructure

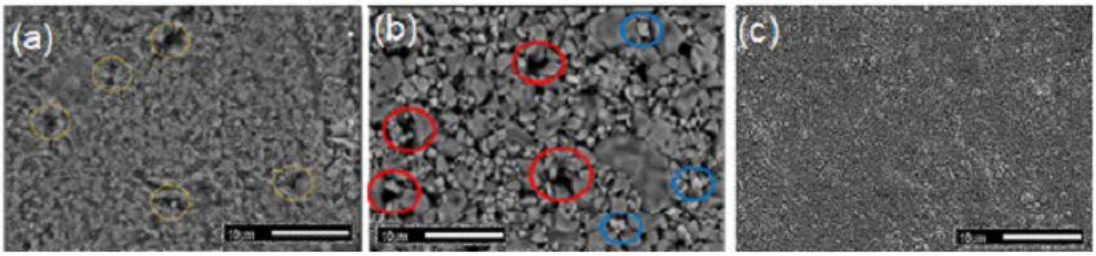

Fig. 4. Microstructure of sintered samples, a) Al_2O_3-monolithic, b) Al_2O_3-1% wt. Ti, c) Compact bone.

Fig 4a and Fig 4b shows the micrographs obtained by Scanning Electron Microscopy, which correspond to the samples sintered at 1500^{o}C with Ti aggregates of 0.0 % and 1 % respectively. In general, it can be observed that the microstructure presents irregularly shaped grains, with sizes smaller than 20µm. When comparing the microstructures, it is possible to observe that the titanium content has an important effect on the microstructure, since the samples with titanium addition present an agglomeration of the grains. On the other hand, it can also be observed in the micrographs the presence of porosity, which was also observed in the alumina matrix, which indicates that this porosity is given by the alumina present in the

samples and this property may favor the growth of a bioactive agent. The circles in red show the areas with higher porosity, which are shown in black in the micrograph. Another important characteristic that can also be noticed in these micrographs is the presence of titanium, which can be observed as small white grains (blue circles). Fig. 4c represents the microstructure of compact bone, in where it's possible to observe a finest gran size in comparison with the microstructure of the samples here processed.

In order to verify the presence of titanium particles in the sample, energy dispersive X-ray analyses were performed. The microstructure where this analysis was carried out, as well as the resulting spectra is shown in Fig. 5, where it is possible to identify that the large gray grains in the microstructure correspond to the alumina matrix, While the small bright particles located in intergranular zones correspond to Ti added to the alumina matrix.

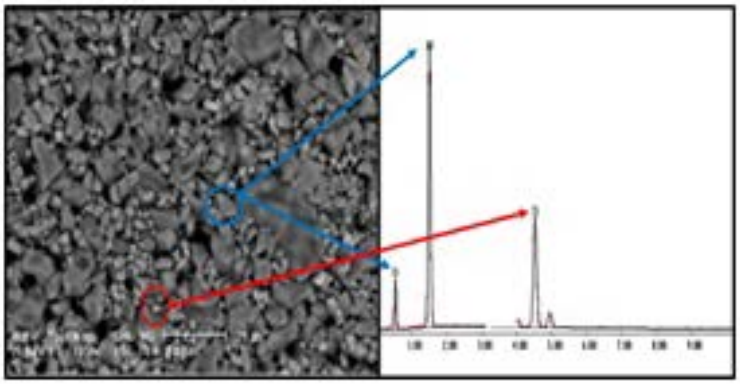

Fig. 5. EDS analysis performed in the Al_2O_3-1% wt Ti sintered sampled.

3.5 Mechanical properties

The mechanical properties evaluated in the fabricated materials are presented in Table I. This table also shows the data for the same properties in compact bone that have been reported in the literature [28].

Tab. I Mechanical properties in composites and compact bone.

Material	**Porosity (%)**	**Elastic modulus (GPa)**	**Micro-hardness (HV)**	**Fracture toughness MPam$^{1/2}$**
Al_2O_3	13 +/- 1	160 +/- 8	575 +/- 16	4.2 +/- 0.1
Al_2O_3-1%Ti	9 +/- 1	253 +/- 13	925 +/- 27	5.7 +/- 0.1
Cortical bone	15	206	350	4.3

As can be seen in this table, the properties of alumina are significantly increased when titanium is added to it. This effect is particularly noticeable in the fracture toughness where the improvement in this property was 135 %. On the other hand, with respect to the properties of the sample Al_2O_3-1 wt.% Ti in comparison with the compact bone, the fracture toughness for Al_2O_3-1 wt.% Ti composite is 132 % higher than that for compact bone. Likewise, the hardness and elastic modulus of the composite are much higher than those of the compact bone. This improvement in the mechanical properties is due to the fact that Ti really acts as a reinforcement material absorbing and dissipating the stresses when the material is under the action of loads. From these results it can be considered that the mechanical properties presented by the Al_2O_3-1 wt.% Ti composite are superior to those of compact bone, so it is

feasible to use this material in the elaboration of synthetic bone for its application as a biomaterial.

3.6 Electrochemical impedance spectroscopy

Fig. 6 shows the electrochemical impedance results in form of Nyquist diagrams (Z_{imag} Vs Z_{real}) for Al_2O_3-1 wt.% Ti composite, considering that composite was immersed in a 0.9 % saline solution. The diagrams in Fig. 6 reveal that the load transfer resistance (Z_{real}) value increases considerably by several orders of magnitude for composites containing 1.0 wt% Ti. This rise in Z_{real} indicates that Al_2O_3-1 wt.% Ti composites is that material that show less degradation in a saline medium similar to the human body. The same Fig. 6 shows the impedance results in the form of Nyquist diagram for the compact bone, which was immersed in a physiological solution in this diagram it is possible to observe a semicircle where the value of load transfer resistance Z_{real} is of the order of 2.800 Ω, which is much lower than the corresponding value of 15.000 Ω of Al_2O_3-1 wt.% Ti composite, which indicates that the bone presents a lower resistance to degradation compared to Al_2O_3-1 wt.% Ti composite.

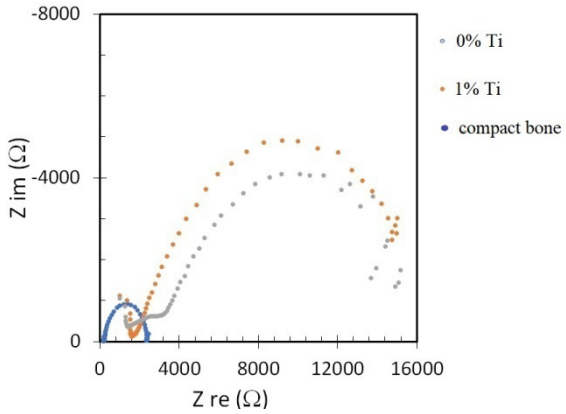

Fig. 6. Nyquist graphs corresponding to the behavior of Al_2O_3-1 wt.% Ti.

3.7 Bioactivity

To promote bioactivity of samples with the titanium aggregates, the biomimetic method was used in which the bioactivity of the compound was demonstrated by the immersion route with the use of a bioactive agent (wollastonite). The evolution of the bioactivity of the sample was demonstrated by X-ray diffraction, where it can be seen how the immersion of the composites in SBF and 1.4SBF favors the formation of hydroxyapatite. Fig. 7 shows the evolution of the samples for 7, 14 and 21 days of testing. In the first 7 days, high peaks corresponding to Ca can be observed in each of the patterns, this is due to the fact that, in the first stage, each of the samples has a light bed of wollastonite ($CaSiO_3$), which is why, when interacting with the sample and with the fluid, be reactions between these two components start. It can also be observed that the first peak, in the standards with sample at 1 % is phosphorus (P). The occurrence of this element is quite important, as there is an indication of the formation of hydroxyapatite, which is the indication that the composite can be called a bioactive material. Hydroxyapatite (Hap) appears in the composites, forming a light layer on them, which will allow bone regeneration. It is also important to mention the formation of some other compounds such as $Ca_2P_2O_7$ or $AlOP_4$, due to the interaction between the samples, the solution and the wollastonite bed.

As mentioned above, the formation of hydroxyapatite ($Ca_5(PO_4)_3(OH)$) is really important, as it shows that the composite is bioactive. We can observe this in the next stage of the biomimetic method (14 days). Here we can already observe a decrease in calcium as an individual compound, but there are more components that include it, as well as phosphorus, which indicates the formation of hydroxyapatite.

As the study progressed, the permanence of phosphorus, an indicator of the presence of hydroxyapatite, can be seen. In the figure 7 (21 days) it can be seen that the pattern having a higher intensity of this element is the Al_2O_3-1 wt.% Ti sample. The formation of different compounds can also be observed, which, as mentioned, are the result of the interactions between the fluid components and the alumina matrix samples with titanium aggregates in different percentages.

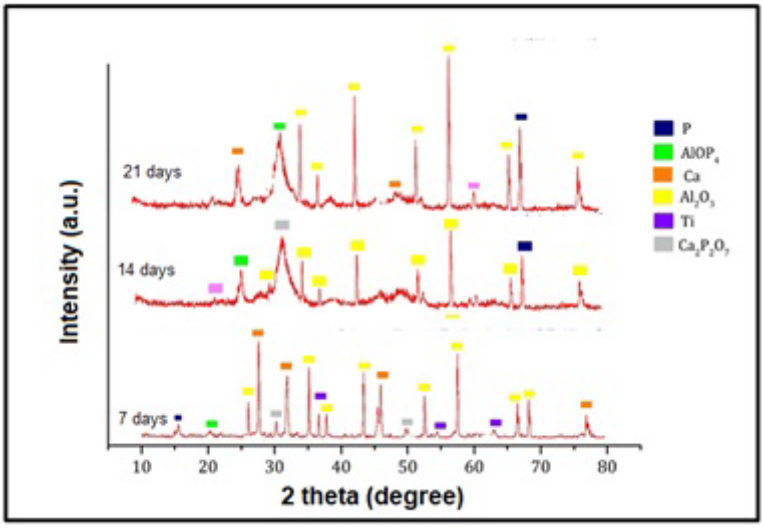

Fig. 7. Bioactivity of the sample followed by X-ray diffraction.

This can be demonstrated by means of an Absorption Spectroscopy (AA) and Plasma Atomic Emission Spectroscopy (ICP) study, carried out in an atomic absorption equipment Thermo Scientific model ICE 3300 and a plasma emission spectrometer Perkin Elmer Model Optima 8300. Using this study, it is possible to determine the amount of each of the elements present only in the fluid remaining in the samples.

In Table II, samples 1-3 correspond to the fluids with unconcentrated SBF. Samples 1 (7 days), 2 (14 days) and 3 (21 days) correspond to the Al_2O_3-1 wt.% Ti. Once the first stage was completed, the liquid is removed from all samples by changing the liquid to 1.4SBF. Samples 5-6 correspond to the second immersion stage (7 days). Sample 4 (14 days) for the same composite. Once the 14 days had passed, the liquid and tablet was removed. Samples 5 are from the third system (21 days). Sample 6 is the last liquid corresponding to the last stage corresponding to the re-immersion (liquid is returned to 1.4 %). Table II shows the main components present in each of the samples. From this, we can observe that in samples 1-2, we see a large presence of calcium, but no phosphorus, and it is in this transition period of 7-14 days, in which there begins to be a proliferation of phosphorus. From samples 3-5, we again see the presence of calcium and phosphorus, since there is already beginning to be an activation of the material, allowing the growth of hydroxyapatite, which is why there, is beginning to be an amount of calcium and phosphorus. Although, the amounts are not as large as those at the beginning, their presence is important, as they indicate growth on the surface of the sample, which is more important. It is also significant to note that the amounts of aluminum and titanium are quite low, since most of them are present in the samples and not in the fluids.

Tab. II Chemical composition of remaining fluids of biomimetic method by AA and ICP.

Sample	Ca (mg/l)	P (mg/l)	Al (mg/l)	Ti (mg/l)
1	564.7	<0.10	<0.10	<0.10
2	557.30	<0.10	<0.10	<0.10
3	573.80	<0.10	<0.10	<0.10
4	90.20	0.374	<0.10	<0.10
5	134.0	<0.10	<0.10	<0.10
6	6.14	27.46	<0.10	<0.10

4. Conclusion

- In this work an Al_2O_3-1 wt.% Ti composite was successfully manufactured through powder techniques.
- The obtained material presents similar mechanical properties (HV, K_{IC}, E) to the properties of compact bone.
- The electrochemical impedance spectroscopy study, indicate that 1 wt.% Ti additions on Al_2O_3 improve the corrosion resistance of the composite in saline media similar to that of the human body.
- The use of the biomimetic method for bioactivation of an Al_2O_3-1 wt.% Ti composite is possible after 21 days, when hydroxyapatite begins to proliferate on the surface of the substrates.

5. References

1. C. Ning, Y. Zhou, Biomaterials 23 (2002) 2909.
2. M. Mirković, L. Kljajević, S. Filipović, V. Pavlović, S. Nenadović, Sci. Sint., 52 (2020) 405.
3. A. Cîmpean, F. Miculescu. Eds. Biomaterials and Implant Biocompatibility, MDPI Books, Switzerland, 2020.
4. V. Z. Mališić, N. Z. Tomić, M. M. Vuksanović, B. D. Balanč, Z. M. Stević, A. D. Marinković, R. M. J. Heinemann, S. S. Putić, Sci. Sint., 52 (2020) 457.
5. W. R. Wagnere, S. E. Sakiyama-Elbert, G. Zhang, M. J. Yaszemski, Biomaterials Science An Introduction to Materials in Medicine, 4th ed. Academic Press, Cambridge, Massachusetts, USA (2020).
6. B. Love, Biomaterials, 1st ed. Academic Press, Cambridge, Massachusetts, USA (2020).
7. V. Hasirci, N. Hasirci, Fundamentals of Biomaterials, 1st ed. Springer, Switzerland, (2018).
8. J. K. Wesley,The Handbook of Advamced Materials, Jon Wiley Intersciencie, USA, 2004.
9. K. Yoshida, H. Mishina, S. Sasaki, Mater. Trans. 45 (2004) 3209.
10. H. Mishina, Y. Inumaru, U. Kaitouk, J Jpn I Met Mater 69 (2005) 847.
11. X. Yao, Z. Huanga, L. Chena, A, D. Jianga, S. Tana, D. L. Michel, G. Wang, L. Mazerolles, J. Pasto, Matter. Lett. 59 (2005) 2314.
12. K. Konopka, Powder Metall Met C, 54 (2015) 374.
13. E. Lucchini, S. Casto, O. Sbaizero, Mater. Sci. Eng., 2003: 369-375.
14. G. De Portu, S. Guicciardi, C. Melandri, F. Monteverde, Wear, 262 (2007) 1346.
15. A. Pérez-de la Fuente, E. Rocha-Rangel, J. A. Rodríguez-García, C. A. Hernández Bocanegra, J. Res. Nanotechnol. 2016 (2016) 1.

16. J. G. Jia, T. M. Guo, J. B. Zhang, L. An, j. S. Ji, Q. Ma, Trans. Mats. H. Treat. 34 (2013) 1.
17. E. Picornell-Pérez, Análisis Previo de Biocompatiblidad de un Material Compuesto de Hap-Ti Fabricado por Pulvimetalurgia, Bachelor thesis, Universidad Carlos III de Madrid, Spain, (2013) (In Spanish).
18. A. Maji, G. Choubey, Mater. Today: Proc., 5 (2018) 7457.
19. J. Liu, H. Yan, M. J. Reece, K. Jiang, J. Eur. Ceram. Soc. 32, (2012) 4185.
20. V. Sáenz de Viteri, E. Fuentes, Titanium and Titanium Alloys as Biomaterials. In Tech Open, United Kingdom, 2013.
21. L. I. Wang, X.F. Wang, C.L. Yu, Y.Q. Zhao., Sci. Sint., 47 (2015) 107.
22. N. Claussen, S. Wu, D. Holz, J. Eur. Ceram. Soc, 14 (1994) 97.
23. ASTM B962-17: Standard Test Methods for Density of Compacted or Sintered Powder Metallurgy (PM) Products Using Archimedes' Principle, Pensylvania, USA, 2017.
24. T. Miyoshi, N. Sagawa, T. Sassa, Trans. Jpn. Soc. Mech. Eng. C. 51, (1985) 2489.
25. ASTM C1327-15: Standard Test Method for Vickers Indentation Hardness of Advanced Ceramics, Pensylvania, USA, 2015.
26. ASTM E1876-15: Standard Test Method for Dynamic Young's Modulus, Shear Modulus, and Poisson's Ratio by Impulse Excitation of Vibration, Pensylvania, USA, 2015.
27. T. Kokubo, H. Kushitani, S. Sakka, T. Kitsugi, T. Yamamuro, (1990), J. Biomed. Mater. Res, 24 (1990) 721.
28. S. Ahmed, K. Suvardhan, Handbook of Bionanocomposites, Pan Stanford Publishing Ltd, USA, 2018.

Сажетак: *Композит Al_2O_3-1 wt.% Ti је припремљен из прахова са намером да се анализирају механичка и хемијска својства за употребу као биоматеријал. Алумина је синтетисана употребом реакционог везивања алуминијум оксида (PBAO). Честице праха након млевења су биле испод 1,5 микрона. Уз помоћ рендгенске дифракције и диференцијалне термијске анализе, утврђено је да алуминијум оксидује и у течном и у чврстом стању током PBAO процеса. Такође је утврђено да је реакција формирања алумине завршена на 1100°C. Из мерења механичких својстава (HV, KIC, E) Al_2O_3-1 wt.% Ti композита, установљено је да су ова својства боља него својства саме кости. Електрохемијска импеданс спектроскопија указује на то да додатак 1 wt.% Ti у Al_2O_3 побољшава отпорност на корозију. Биоактивност Al_2O_3-1 wt.% Ti композита је била успешна употребом биомиметичког метода, јер након 21 дана, хидроксиапатит почиње да се размножава на површини супстрата. Са свим овом резултатима можемо закључити да је изводљива употреба Al_2O_3-1 wt.% Ti композита као синтетичке кости и има примену као биоматеријал.*

Кључне речи: *алумина, титанијум, биоактивација, биоматеријал, кост.*